RESEARCH ARTICLE

WILEY

Reduced network integration in default mode and executive networks is associated with social and personal optimism biases

Dominik Andreas Moser[1,2] | Mihai Dricu[1] | Raviteja Kotikalapudi[1] | Gaelle Eve Doucet[3] | Tatjana Aue[1]

[1]Institute of Psychology, University of Bern, Bern, Switzerland

[2]Child and Adolescent Psychiatry, University Hospital Lausanne, Lausanne, Switzerland

[3]Institute for Human Neuroscience, Boys Town National Research Hospital, Omaha, Nebraska

Correspondence
Dominik Andreas Moser, Institute of Psychology, University of Bern
Bern, Switzerland.
Email: domamoser@gmail.com

Abstract

An optimism bias refers to the belief in good things happening to oneself in the future with a higher likelihood than is justified. Social optimism biases extend this concept to groups that one identifies with. Previous literature has found that both personal and social optimism biases are linked to brain structure and task-related brain function. Less is known about whether optimism biases are also expressed in resting-state functional connectivity (RSFC). Forty-two participants completed questionnaires on dispositional personal optimism (which is not necessarily unjustified) and comparative optimism (i.e., whether we see our own future as being rosier than a comparison person's future) and underwent a resting-state functional magnetic resonance imaging scan. They further undertook an imaginative soccer task in order to assess both their personal and social optimism bias. We tested associations of these data with RSFC within and between 13 networks, using sparse canonical correlation analyses (sCCAs). We found that the primary sCCA component was positively connected to personal and social optimism bias and negatively connected to dispositional personal pessimism. This component was associated with (a) reduced integration of the default mode network, (b) reduced integration of the central executive and salience networks, and (c) reduced segregation between the default mode network and the central executive network. Our finding that optimism biases are linked to RSFC indicates that they may be rooted in neurobiology that exists outside of concurrent tasks. This poses questions as to what the limits of the malleability of such biases may be.

KEYWORDS

optimism, resting state, social optimism, social cognition, network connectivity

1 | INTRODUCTION

Optimism refers to the tendency to expect positive rather than negative outcomes. A personal optimistic bias is the overestimation of the likelihood of desirable events happening to oneself, while potentially also underestimating the likelihood of undesirable events happening (Weinstein, 1980). The concept of social optimism bias extends this into social psychology: An individual displaying a social optimism bias overestimates the likelihood of desirable events happening to members of groups one identifies with or that one thinks positively of, while underestimating the likelihood for members of groups one does not identify with or thinks negatively of (Aue, Nusbaum, & Cacioppo, 2012; Dricu et al., 2018).

Studies on brain structure suggest that not only personal but also social optimism bias have a permanent neuronal signature that overlaps with three of the most common networks linked to higher cognition (Chowdhury, Sharot, Wolfe, Düzel, & Dolan, 2014; Dolcos, Hu, Iordan, Moore, & Dolcos, 2016; Moser, Dricu, Wiest, Schupbach, & Aue, 2020). These networks include the default mode network (DMN), the central executive network (CEN), and the salience network (SAL). The DMN is generally thought to serve unspecific inner thought and self-referential processing (Andrews-Hanna, 2012;

Raichle et al., 2001) and includes midline regions such as the ventral anterior cingulate cortex (ACC), ventromedial prefrontal cortex (vmPFC), and dorsomedial prefrontal cortex (dmPFC), but also regions in the posterior cingulate, the precuneus, and the medial and lateral temporal cortices. The CEN—which is generally antagonistic to the DMN (Fox et al., 2005)—subserves many task-dependent functions that necessitate stimulus-dependent attention and cognition (Menon & Uddin, 2010). Regions of the CEN include the lateral frontal and parietal cortex, as well as subcortical areas such as the thalamus and the caudate nuclei. The SAL is involved in evaluating the importance of a stimulus and also plays a crucial role in the transition from states favouring the DMN over the CEN and vice versa (Bolton et al., 2020). The insula, as well as the putamen and dorsal ACC, are included in the SAL (see Figure 1).

Previous studies on grey matter measures linked personal optimism biases to midline and other DMN regions, as well as to regions of the CEN and SAL such as the insula (Chowdhury et al., 2014; Dolcos et al., 2016; Yang, Wei, Wang, & Qiu, 2013). Notably, a recent study further revealed that such structural brain-behaviour associations are not restricted to the personal domain, but extend into the social domain (Moser et al., 2020). Among other results, grey matter thickness of the SAL and CEN regions (such as the insula and inferior
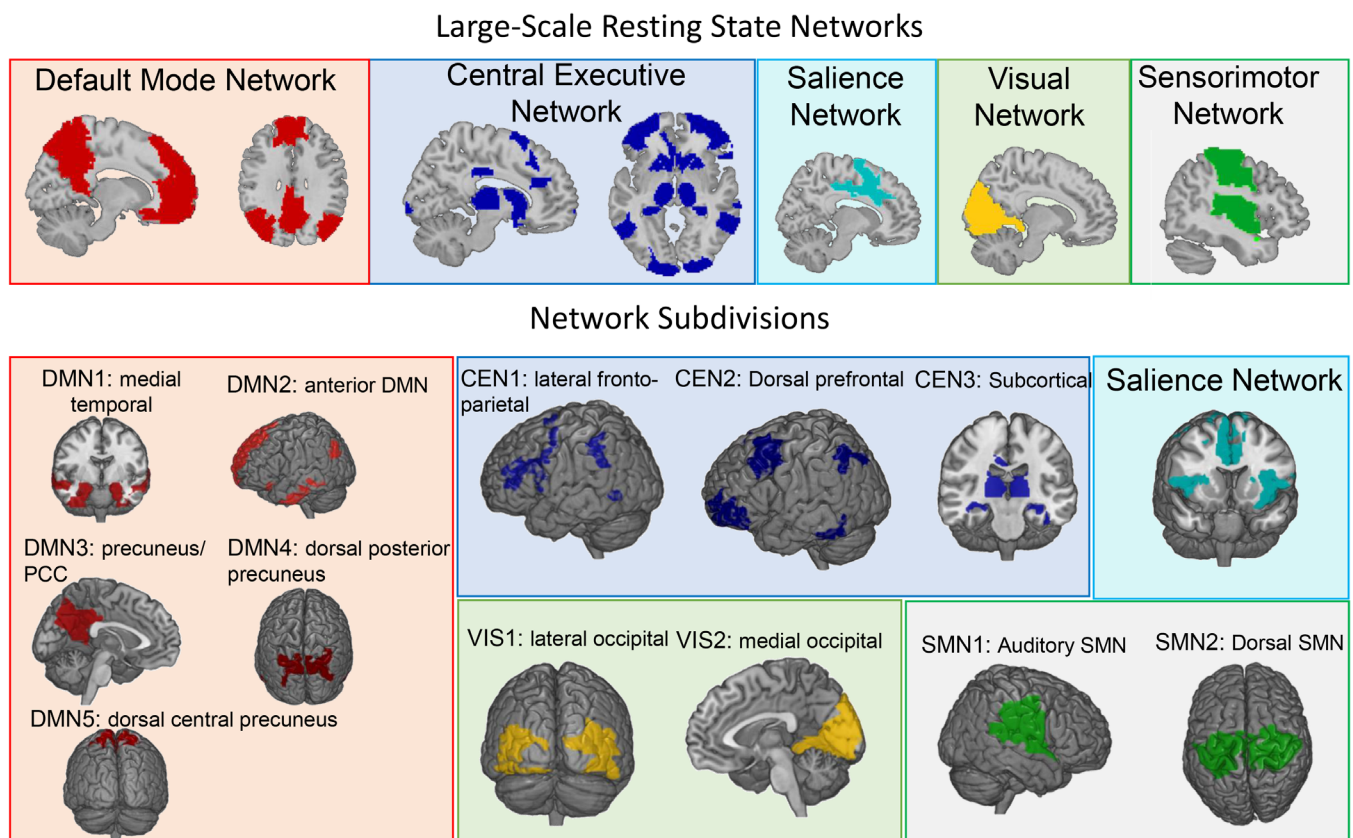

FIGURE 1 Large-scale resting-state networks (a) and their subdivisions (b) used in the present article in accordance with Doucet, Rasgon, McEwen, Micali, and Frangou (2018). Top: Large-scale resting-state networks. Bottom: Subdivisions that make up these large-scale resting-state networks. CEN, central executive network; DMN, default mode network; SMN, sensorimotor network; PCC, posterior cingulate cortex; VIS, visual network. Each colour reflects a specific large-scale resting-state network and its subdivisions

frontal gyrus; IFG) and of the DMN regions (such as the dmPFC) were shown to be associated with less favourable expectations towards out-groups that are perceived as cold. IFG white matter connectivity with subcortical regions was further found to be associated with the size of the belief update bias (Moutsiana, Charpentier, Garrett, Cohen, & Sharot, 2015), which refers to the degree to which we more readily integrate feedback into (personal) future expectations that suggest the need to be more optimistic (rather than pessimistic). The IFG is at a junction of the SAL, the CEN, and the DMN (Doucet, Lee, & Frangou, 2019). It has been suggested that the anterior insula/IFG plays a critical role in the transition of function between the CEN and the DMN (Menon & Uddin, 2010).

In addition, functional studies have shown that both personal and social optimism biases, as well as related concepts (e.g., dispositional optimism), are linked to neural activation and resting-state functional connectivity (RSFC) (Aue et al., 2012; Dricu, Schupbach, et al., 2020; Dricu, Kress, & Aue, 2020;Ran et al., 2017; Wang et al., 2018). Although no studies on optimism bias have been conducted on RSFC at a network level, two of them have investigated brain regions within networks (Ran et al., 2017; Wang et al., 2018). For instance, a resting-state functional magnetic resonance imaging (rs-fMRI) study revealed that dispositional optimism was associated with decreased RSFC between the vmPFC and the IFG, as well as increased RSFC between the vmPFC and the middle temporal gyrus (Ran et al., 2017). Another study indicated that dispositional optimism correlated with spontaneous activity in the orbitofrontal cortex, as well as with RSFC between the orbitofrontal cortex and the supplementary motor cortex (Wang et al., 2018). Moreover, another rs-fMRI study found that regional homogeneity—a measure with a close relationship to local connectivity—was positively correlated with dispositional optimism in several DMN regions, including the dmPFC (Wu et al., 2015).

Finally, Singh et al. (2020) examined attention in relation to optimism and network functional neural activity. They found that asymmetries in the way that participants varied their attention deployment in response to optimistic compared with pessimistic expectations was linked to the way the SAL and CEN were asymmetrically activated during optimistic and pessimistic expectancies (Singh et al., 2020). This finding further indicates that a network approach may be useful in the investigation of optimism-related concepts.

To our knowledge, no fMRI studies have yet investigated different optimism concepts in relation to network RSFC (as opposed to region-of-interest RSFC approaches). In this context, we aimed in the present study to fill a gap in the current literature, wherein the neural underpinnings of social optimism biases in particular remain largely unprobed. Specifically, to our knowledge, the association between RSFC and social optimism biases has never been investigated, nor has it been put in the context of the association between RSFC and personal optimism bias. This gap is noteworthy, as remaining unanswered is the question of the degree to which our tendencies to have different expectations for others is based on task-independent brain connectivity patterns (such as are measured by resting state patterns) as opposed to activation that depends on a specific task at hand. Moreover, examining the links between RSFC and both personal and social

forms of optimism bias in the same study may aid in determining the degree to which these patterns of associations are similar.

To address these aims, we recruited a sample of students who underwent a behavioural task that targeted concepts related to personal and social optimism bias before undergoing an rs-fMRI scan. During the behavioural task, participants were instructed to estimate a soccer player's likelihood of successfully passing the ball to a fellow team player in different situations. They had to do this for four different characters: themselves, a personal rival, a player from their favourite team, and a player from their favourite team's arch-rival. The degree to which they attributed higher chances of successful passes to the self (favourite team) compared with the rival (favourite team's arch-rival) was our measure of personal (social) optimism bias. The participants in addition completed questionnaires that targeted related concepts, namely dispositional personal optimism and comparative optimism (Dricu, Kress, & Aue, 2020). Dispositional optimism refers to an individual's tendency to see the future generally (not situationally bound) in bright colours, which is not necessarily unjustified. Comparative optimism, in contrast, is a form of unrealistic personal optimism and describes an individual's tendency to anticipate a better personal future across a variety of precisely formulated situations than the future of a comparison person of the same age and gender. Comparative optimism therefore also constitutes an optimistic bias.

We used sparse canonical correlation analysis (sCCA) to assess associations of personal and social optimism biases with RSFC between and within brain networks. This method uses an algorithm to assess the association between two data sets that include (a) the different optimism measures and (b) the different RSFC measures. To achieve this, the algorithm groups variables from the two data sets into dimensions (modes). It also assigns weights to the variables constituting each mode in order to determine their respective contributions to the overall association between the optimism data and RSFC data. The use of sCCAs allowed us to take a mostly data-driven approach, which included networks from the entire brain, rather than only those networks that had been the focus of prior findings, such as the CEN, SAL, and DMN. Canonical correlation analyses are a novel but increasingly used method in neuroimaging (for an overview, see (Zhuang, Yang, & Cordes, 2020). The purpose of sCCAs is to provide information about whether one data set associates with another (as opposed to more classic methods such as multiple regression, which associate a number of variables with a single outcome measure). To do this, the algorithm assigns weights to each variable. For each participant, individual measure scores are then multiplied by these weights and summed to an overall score (referred to here as a variate) for each data set. The two variates are then correlated. It may be of interest that weights for the measures of each data set are not assigned blindly by the algorithm (i.e., without knowledge of the other data set).

Using this statistical approach, we expected to find (H1) a significant association of the overall RSFC data set and the optimism data set. (H2) If this were the case, we assumed that an association would be reflected in both sCCAs, focusing on between-network functional connectivity (BNFC) and within-network functional connectivity

(WNFC), respectively. (H3) In addition, we hypothesised, that—if such an association existed—it would, like our previous finding on brain structure, point towards a shared neural correlate of both social and personal optimism biases (Moser et al., 2020). (H4) In accordance with the existing literature on optimism and FC, we expected that a neural correlate or optimism would be revealed in both WNFC and BNF and include the SAL, CEN, and DMN (Ran et al., 2017; Wang et al., 2018; Wu et al., 2015).

2 | METHODS

Participants: Forty-nine healthy German-speaking candidates were recruited, between 18 and 35 years of age (age [mean ± std] = 22.87 ± 3.62 years, 34 females), none of whom played soccer. Recruitment was made through emails, flyers, and the local participant pool at the University of Bern, Switzerland.

Exclusion criteria included self-reported neurological conditions, psychoactive substance usage, and left-handedness, as well as ability to enter an MRI machine. Participation was compensated with either course credits or 25 Swiss francs per hour. Participants gave written informed consent, in accordance with the guidelines of the Declaration of Helsinki (World Medical Association, 2013). Experimental procedures were approved by the local ethics committee of the University of Bern, Switzerland. In the end, 42 participants were included. Five participants were excluded due to excessive head motion (see detail on quality control below) during the resting state fMRI scan and two for being outliers (>3 SD difference from the mean) on more than 10 measures (see details of the measures in next section).

Experimental procedure and measures of the behavioural task: The experiment took place in the scanner and lasted about 30 min (task fMRI data were not analysed due to technical problems). Each participant saw four different animated characters, representing different soccer players, playing in 24 identical football scenarios that were adapted from a similar experiment on American football (Aue et al., 2012) and tested in behavioural experiments prior to the present study. Participants were given specific instructions and training prior to the experiment (see Supplementary Materials for further information). Characters were created with *The Sims 4* (Electronic Arts, California). These characters represented (a) the participants themselves (b) a rival with similar talent and competence, (c) an unknown player of a team that they identified with/desired to join shortly (in-group), and (d) an unknown player of the arch-rival team (out-group). The 16 soccer scenarios were created as pictures in Photoshop CS6 (Adobe Inc.). The participants' task was to estimate a player's likelihood of successfully passing the ball to a fellow team player. For this likelihood judgement, participants were given an analogue-looking scale on which they could move the indicator via button press. The task was performed in two blocks (a + b and c + d) with randomised trials (n = 24 per character). For each participant, task scores (assigned likelihood of pass success, ranging from 0% [certain that the pass will not be successful] to 100% [certain that the

pass will be successful]) were averaged across trials for each character. From these likelihood averages, we estimated relative biases that is, personal optimism bias and social optimism bias (see Figure 2) calculated as follows: personal optimism bias = self – rival; social optimism bias = in-group – out-group. In addition to personal and social optimism biases, we also calculated valence and relevance biases (see Figure 2): valence bias = [self + in-group] – [rival + out-group]; relevance bias = [self + rival] – [in-group + out-group]. Valence bias is the combination of personal and social optimism bias and is therefore useful as a generalised measure of task-related optimism biases independent of whether the judgement is personally or socially relevant to the participant. Relevance is the orthogonal concept of valence. It was included as a general measure of how important the social factor is independently of valence. Specifically, relevance refers to the difference between individual and social factors. Inclusion of these two measures therefore allowed us to judge whether more generalised biases were at the origin of effects observed for our more specific optimism biases.

In addition, the participants completed a sociodemographic questionnaire and measures of personal (i.e., self-related) optimism, including the German versions of the Comparative Optimism Scale (COS; Weinstein, 1980) and the Revised Life Orientation Test (LOT-R; Glaesmer, Hoyer, Klotsche, & Herzberg, 2008; Scheier, Carver, & Bridges, 1994). Questionnaires were filled in by using an online portal following the MRI scan. The COS measures self-related future expectancies as compared with another person of the same age and gender and thus also personal optimism bias. In the present sample, Cronbach's alpha for internal consistency was 0.75 for the COS optimism subscale and 0.81 for the COS pessimism subscale. The LOT-R was used to measure dispositional optimism, that is, the disposition to have an optimistic life orientation (good things being likely to happen) that does not necessarily have to be unrealistic. Cronbach's alpha for the LOT-R optimism scale was 0.69 for the optimism subscale and 0.68 for the pessimism subscale (Glaesmer et al., 2008). Each of these two measures has an optimism and a pessimism subscale, the latter subscales measuring the extent to which people anticipate their future to hold undesirable outcomes. Both subscales of the questionnaires were included in this study.

MRI scan: For each participant, MRI data were collected on a 3 T scanner (MAGNETOM Prisma, Siemens, Erlangen, Germany) using a 64-channel head coil, at the Inselspital, University Hospitals Bern, Switzerland. The structural scan used a 3D Magnetization Prepared Rapid Gradient Echo (MPRAGE or T1-weighted) sequence with repetition time (TR) = 2,300 ms, echo time (TE) = 2.98 ms, inversion time (TI) = 900 ms, flip angle = 9°, matrix size = 160 × 256 × 256 with an isotropic spatial resolution = 1 mm³. The resting state fMRI scan included 1,000 acquisitions with 32 slices, TR = 300 ms, TE = 30 ms, flip angle = 30°, field of view = 230 mm with an isotropic spatial resolution = 3.6 mm³ and a multi-band acceleration factor of 8. Participants were instructed to stay still and keep their eyes open.

Resting state MRI pre-processing: Pre-processing was performed with SPM12 (www.fil.ion.ucl.ac.uk/spm/software/spm12/) and DPABI (Yan, Wang, Zuo, & Zang, 2016) toolboxes in MATLAB R2017
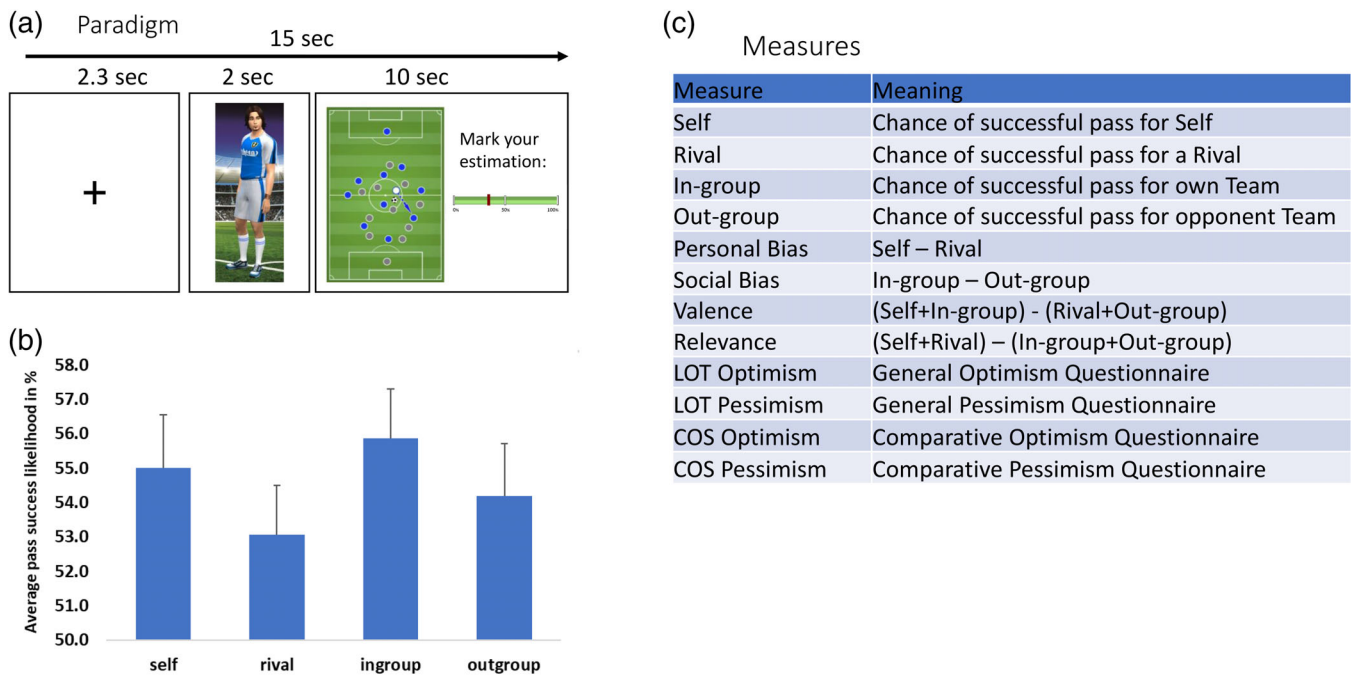
(a) Paradigm

(b)

(c) Measures

Measure	Meaning
Self	Chance of successful pass for Self
Rival	Chance of successful pass for a Rival
In-group	Chance of successful pass for own Team
Out-group	Chance of successful pass for opponent Team
Personal Bias	Self – Rival
Social Bias	In-group – Out-group
Valence	(Self+In-group) - (Rival+Out-group)
Relevance	(Self+Rival) – (In-group+Out-group)
LOT Optimism	General Optimism Questionnaire
LOT Pessimism	General Pessimism Questionnaire
COS Optimism	Comparative Optimism Questionnaire
COS Pessimism	Comparative Pessimism Questionnaire

FIGURE 2 Paradigm and measures. (a) Cartoon of the paradigm with timeline. (b) Results of average likelihood given to each character of the paradigm. Error bars indicate standard error. (c) Summary of all non-imaging measures entered into the analysis. LOT, Revised Life Orientation Test; COS, Comparative Optimism Scale

(MathWorks). All DICOM images were converted to NIfTI format by using dcm2niix (https://github.com/rordenlab/dcm2niix/releases). The first five volumes were excluded. Using rigid-body alignment, resting-state fMRI data were motion corrected to the first volume; we performed cross-modality co-registration between the functional scans and the anatomical T1 scan, spatial normalisation of the functional images into Montreal Neurological Institute stereotaxic standard space, and spatial smoothing with a 6-mm full-width at half-maximum Gaussian kernel. Further steps were applied: wavelet despiking (Patel et al., 2014), detrending, and multiple regression of motion parameters and their derivatives (24-parameter model; Friston, Williams, Howard, Frackowiak, & Turner, 1996), as well as white matter-cerebrospinal fluid time series and their linear trends by using the CompCor noise reduction method (five principal components; Behzadi, Restom, Liau, & Liu, 2007). Lastly, data were bandpass filtered to 0.01–0.1 Hz (Cordes et al., 2001). In order to ensure that no RSFC results were related to head motion (Power, Barnes, Snyder, Schlaggar, & Petersen, 2012), we chose stringent threshold and exclusion criteria. Data sets were excluded if volume-to-volume head motion was above 0.5 mm in more than 0.2% of all scans. After we excluded five participants, the mean (SD) framewise displacement was 0.08 mm (SD = 0.02).

FC analysis: The networks were derived from a previously established and reproducible brain functional atlas of 13 networks based on rs-fMRI data from 496 participants (Doucet et al., 2018; Doucet et al., 2019). That atlas was chosen because it is reproducible (Doucet et al., 2019) and a good compromise in terms of spatial resolution. The partition includes common resting state networks and

subdivisions, including five higher-order networks: DMN: five networks, SAL: one network, CEN: three networks, sensorimotor (SMN): two networks, and visual (VIS): two networks (Figure 1). For each network, we computed Fisher's Z-transformed Pearson's correlation coefficients as measures of within-network (cohesiveness) and between-network (integration) FC.

Within-network FC (cohesiveness) was computed as the average correlation of each voxel's BOLD signal time series with every other voxel within the network. Between-network FC (network integration) was computed as the correlation between the average time series of each pair of networks. This analysis led to 13 measures of network cohesiveness and 78 measures of network integration per participant.

2.1 | Statistical analyses

(Sparse) canonical correlation analysis (sCCA): In order to determine the relationship between RSFC and the optimism-related measures, we used an sCCA approach with an L1-norm penalty (Witten, Tibshirani, & Hastie, 2009), using a MATLAB script available online (Ing et al., 2019). The purpose of sCCA is to provide information about whether one data set associates with another. To do this, sCCA specifies linear combinations (pairs of canonical variates) of variables in optimism data and variables in the RSFC data set that best express the maximal correlation (i.e., canonical correlation) between the two data sets. Each variable is given a weight that it contributes to the variate that represents the data set it belongs to. The correlations between the canonical variates are the canonical correlations. For this,

the algorithm groups variables from either side into component pairs/dimensions, which are referred to as modes in the present paper.

Prior to analysis, age, sex, and body mass index were regressed out of both data sets, and potential outlier values (>3 *SD* below or above mean) were removed and replaced by mean values. Instead of a classic (non-sparse) canonical correlation analysis, we conducted sCCA because this analysis (a) permits the inclusion of more variables than participants and (b) allows stronger inferences regarding the contribution of individual variables (for similar approaches, see Moser et al., 2017; Moser et al., 2018). The FC measures were combined in three different RSFC data sets: (a) an all RSFC data set, with 91 network connectivity measures to allow a general overview (this is the primary analysis of the study and yields a single omnibus significance value for the entire analysis); (b) a BNFC data set with 78 measures; and (c) a WNFC data set with 13 measures. The latter two analyses were aimed at allowing more specific focuses and served to further investigate concrete BNFC and WNFC origins of the initial sCCA conducted. Hence, for each of these data sets, one sCCA was computed.

For mode 2 and following, each mode associates the personal and social optimism data with the FC after having regressed out the variance that was already explained by all previous modes (components). Therefore, the explained variance tends to get smaller with each subsequent mode. We calculated the first 10 sCCA modes to determine the variance explained in one variate by the variate of the other data set. Following the calculation of those 10 modes, we then restricted permutations and reliability analyses to the first seven modes, as later modes did not explain more than 2% of the variance. We determined significance by using 5,000 permutations. The threshold for statistical significance was set at $p < .05$. We then extracted the weights of the variables contributing to both variates in each mode and report variables with weights of more than 0.1 in the main text. Kolmogorov–Smirnov tests did not reject normality for any of the data as it was entered.

Reliability analyses: Reliability analyses were performed in MATLAB and included the following:

1. In order to ensure that the results were not dependent on the atlas used, we also conducted the analyses by using the Consensual Atlas of Resting-state Network (CAREN), which combines several other resting-state-derived network atlases (Doucet et al., 2019).

2. Leave-one-out analyses for each participant by using an in-house script.

3. We examined the reliability of the overall sCCA correlation as a function of sample size by using 1,000 different bootstrapping iterations of the existing sample, testing for sample sizes from 10% of the current sample to 300% the size of the current sample.

4. Mean and standard deviation of the redundancy-reliability score (Moser's RR-score) for each mode (Moser et al., 2018). The RR-score is a measure of the stability of the variable-to-variate correlations and indicates whether results can be expected to be reliable independent of sample composition. The RR-score is based on a training-test set approach and essentially measures whether test sets have similar associations between variables and variates, whereby results with high RR-scores can be assumed to be truly carried by the entire sample and not to be dependent on a specific subset of the population that may not be reliably reproduced if one were to replicate the study (Moser, 2018; Moser et al., 2018). In the present study, 5,000 splits of training and test sets were performed in order to calculate the mean RR-score.

Post hoc analyses: In order to allow comparison with more traditional analysis techniques (e.g., meta-analyses) and to enable dedicated readers to get a better grasp on the origin of the effects found in sCCA, we also included univariate analyses, that is, correlations as part of a supplementary data set. For brevity, the main manuscript describes only univariate results that are related to the main findings and that may better describe the origins of the sCCA findings.

3 | RESULTS—BEHAVIOURAL ANALYSES

Questionnaire and task data: The likelihood of pass success for the different characters were as follows: Self: mean = 55.0%, *SD* = 10.0%; rival: mean = 53.1%, *SD* = 9.2%; in-group: mean = 55.9%, *SD* = 9.3%; out-group: mean = 54.2%, *SD* = 9.8%. Paired t-tests suggested differences between the rival and both the self ($p = .022$) and the in-group ($p = .002$), as well as between the in-group and the out-group ($p = .011$). Calculated bias measures were as follows: personal bias: mean = 1.9%, *SD* = 5.2%; social bias: mean = 1.7%, *SD* = 4.0%; valence bias: mean = 3.6%, *SD* = 7.5%; relevance bias: mean = −2.8%, *SD* = 5.4%. Mean questionnaire values for optimism and pessimism were as follows: for the LOT-R, optimism: mean = 8.81, *SD* = 2.00; pessimism: mean = 3.76, *SD* = 1.90; for the COS, optimism: mean = 70.7, *SD* = 10.1; pessimism: mean = 76.1, *SD* = 13.5. Means and distributions of the RSFC variables are available in Table S1 (Supporting information).

4 | RESULTS—RESTING-STATE FC

sCCA for all RSFC and optimism data: The first mode of the sCCA was significant ($p = .033$). None of the other modes reached significance ($p > .06$). In the optimism data set, the highest positive weights were given to valence (weight = 0.51), social optimism (weight = 0.48), and personal optimism (weight = 0.39) biases, followed by the LOT optimism subscale (weight = 0.26) and the likelihood for successful passes for the self (weight = 0.26) and the in-group (weight = 0.21). In contrast, the LOT pessimism subscale (weight = −0.33) and the relevance bias (weight = −0.22) negatively contributed to the RSFC data set (see Table 1 and Figure 3). In the RSFC data set, sizeable positive weights (>0.2) were given exclusively to network integration measures (between-network FC): FC between the CEN1 and three other networks (DMN1: weight = 0.22; DMN3: weight = 0.30; CEN2: weight = 0.21), as well as FC between the SMN1 and the SMN2 (weight = 0.22). The most important negative weights were given to WNFC within DMN1 (weight = −0.32) and FC between CEN3 and three other networks (CEN1: weight = −0.21; CEN2: weight = −0.20; DMN4: weight = −0.33), as well as FC between the SAL and CEN1 (weight = −0.26) (see Table 2 and Figure 3).

TABLE 1 Sparse canonical correlation analysis for all resting-state network functional connectivity: mode 1 weights for the behavioural variate

Measure	Weight
Valence bias	0.512
Social bias	0.478
Personal bias	0.390
Self success likelihood	0.264
LOT optimism	0.256
In-group success likelihood	0.206
COS pessimism	0.103
COS optimism	0.083
Rival success likelihood	0.068
Out-group success likelihood	−0.015
Relevance bias	−0.216
LOT pessimism	−0.332

Abbreviations: COS, Comparative Optimism Scale; LOT, Life Orientation Test.

(weight = 0.51) and personal (weight = 0.43) and social optimism biases (weight = 0.42), followed by the likelihood for successful passes for the self (weight = 0.32) and the in-group (weight = 0.25), as well as the LOT optimism subscale (weight = 0.24). The LOT pessimism subscale (weight = −0.27) and the relevance bias (weight = −0.23) contributed with negative weights (see Tables 3 and 4 and Figure 3). Concerning weights for BNFC, positive weights were given for connectivity between the CEN1 and four other networks (DMN1: weight = 0.25, DMN2: weight = 0.22, DMN3: weight = 0.34, CEN2: weight = 0.24). Post hoc univariate analyses indicated that these findings were primarily driven by positive correlations of BNFC and personal and social optimism biases, as well as the valence bias, and by negative correlations of BNFC with the relevance bias (see Data S1 and Figure S2). In addition, two BNFC connectivity measures involving the SMN had important positive weights (SMN1-SMN2: weight = 0.23, SMN2-DMN5: weight = 0.20), as well as the DMN4-VIS2 connectivity (weight = 0.22). Post hoc univariate analysis indicated that the DMN4-VIS2 finding was primarily driven by a negative correlation of BNFC with the relevance bias (see Data S1). Negative
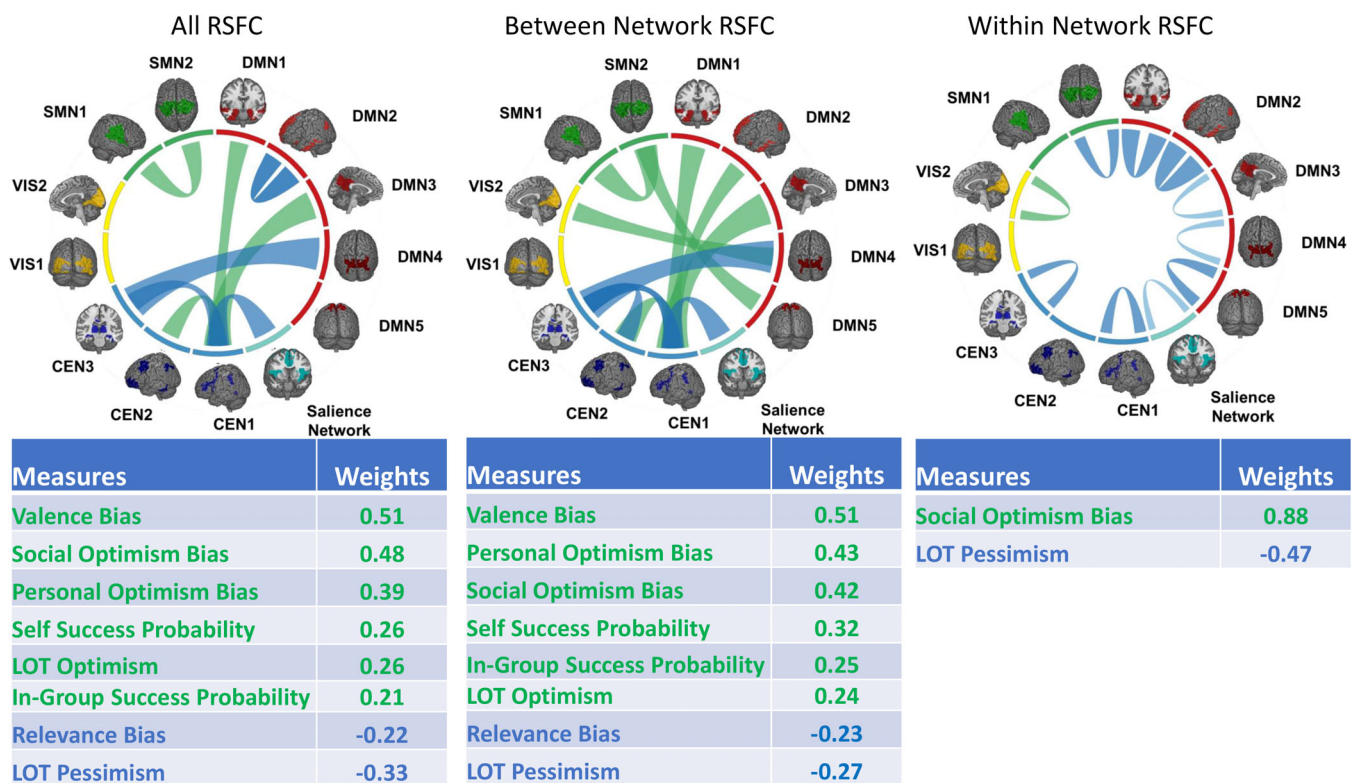

FIGURE 3 Mode 1 of three sparse canonical correlation analyses using an optimism data set and three different functional connectivity data sets. Only weights above 0.2 are shown. Green connections are positive weights, blue connections are negative weights. CEN, central executive network; DMN, default mode network; LOT, Revised Life Orientation Test; RSFC, resting-state functional connectivity; SMN, somatosensory network; VIS, visual network

sCCA for the BNFC data set and optimism data: The first mode of the sCCA was significant (p = .0216); none of the other modes reached significance (p > .10). Similar to the sCCAs for all RSFC, the highest positive weights in mode 1 were given to valence

weights were given exclusively to BNFC among the CEN and SAL networks (CEN1-CEN3: weight = −0.22, CEN1-SAL: weight = −0.26, CEN2-CEN3: weight = −0.21) with the exception of BNFC between CEN3 and DMN4 (weight = −0.36). Post hoc univariate analysis

Connectivity	Network 1	Network 2	Weight
Between	CEN1 lateral frontoparietal	DMN3 precuneus/PCC	0.302
Between	SMN1 auditory SMN	SMN2 dorsal SMN	0.218
Between	DMN1 medial temporal	CEN1 lateral frontoparietal	0.215
Between	CEN2 dorsal prefrontal	CEN1 lateral frontoparietal	0.211
Between	VIS2 medial occipital	DMN4 dorsal posterior precuneus	0.194
Between	DMN2 anterior DMN	CEN1 lateral frontoparietal	0.191
Between	DMN5 dorsal central precuneus	SMN2 dorsal SMN	0.170
Between	Salience	DMN2 anterior DMN	0.157
Between	DMN4 dorsal posterior precuneus	SMN2 dorsal SMN	0.103
Between	DMN2 anterior DMN	DMN3 precuneus/PCC	−0.100
Within	SMN2 dorsal SMN		−0.117
Within	CEN1 lateral frontoparietal		−0.123
Between	CEN2 dorsal prefrontal	DMN2 anterior DMN	−0.125
Between	DMN2 anterior DMN	DMN4 dorsal posterior precuneus	−0.128
Between	DMN5 dorsal central precuneus	SMN1 auditory SMN	−0.135
Between	Salience	DMN4 dorsal posterior precuneus	−0.141
Between	DMN1 medial temporal	DMN2 anterior DMN	−0.154
Between	SMN1 auditory SMN	CEN1 lateral frontoparietal	−0.167
Within	DMN1 medial temporal		−0.177
Between	CEN2 dorsal prefrontal	CEN3 subcortical	−0.197
Between	CEN3 subcortical	CEN1 lateral frontoparietal	−0.214
Between	Salience	CEN1 lateral frontoparietal	−0.256
Within	DMN2 anterior DMN		−0.323
Between	DMN4 dorsal posterior precuneus	CEN3 subcortical	−0.330

TABLE 2 Sparse canonical correlation analysis for all resting-state network functional connectivity: mode 1 weights for the resting-state connectivity variate

Note: Only absolute weights >0.1 shown.
Abbreviations: CEN, central executive network; DMN, default mode network; PCC, posterior cingulate cortex; SMN, sensorimotor network; VIS, visual network.

TABLE 3 Sparse canonical correlation analysis for between-network resting-state functional connectivity: mode 1 weights for the behavioural variate

Measure	Weight
Valence bias	0.508
Personal bias	0.429
Social bias	0.423
Self success likelihood	0.319
In-group success likelihood	0.251
LOT optimism	0.239
Rival success likelihood	0.106
COS pessimism	0.101
COS optimism	0.099
Out-group success likelihood	0.052
Relevance bias	−0.227
LOT pessimism	−0.268

Abbreviations: COS, Comparative Optimism Scale; LOT, Life Orientation Test-Revised.

indicated that these results were jointly driven by negative correlations of BNFC and the personal and social optimism biases, as well as the valence bias, and positive correlations of BNFC with the LOT pessimism subscale and the relevance bias (see Data file).

sCCA for WNFC and optimism data: Modes 1 (p = .0272) and 3 (p = .016) were significant. None of the other tested modes were significant (p > .15). For the mode 1 behavioural variate, a positive weight was given to social optimism bias (weight = 0.88) and a negative weight to the LOT pessimism subscale (weight = −0.47). In terms of mode 1 and WNFC, a strong (weight > 0.2) positive weight arose for the VIS2 network, whereas negative weights appeared for two CEN networks (CEN1: weight = −0.29, CEN3: weight = −0.24), three different DMN networks (DMN1: weight = −0.44, DMN2: weight = −0.56, DMN5: weight = −0.30), and the dorsal SMN2 (weight = −0.30; see Table 5 and Figure 3). Post hoc univariate analyses indicated that findings in the DMN, CEN, and SMN were driven by both positive associations of WNFC with the LOT pessimism subscale and negative associations with the social optimism bias, while the inverse was true for the VIS finding (see Data S1).

TABLE 4 Sparse canonical correlation analysis for between-network resting-state functional connectivity: mode 1 weights for the resting-state functional connectivity variate

Network 1	Network 2	Weight
CEN1 lateral frontoparietal	DMN3 precuneus/PCC	0.335
DMN1 medial temporal	CEN1 lateral frontoparietal	0.245
CEN2 dorsal prefrontal	CEN1 lateral frontoparietal	0.241
SMN1 auditory SMN	SMN2 dorsal SMN	0.232
VIS2 medial occipital	DMN4 dorsal posterior precuneus	0.224
DMN2 anterior DMN	CEN1 lateral frontoparietal	0.219
DMN5 dorsal central precuneus	SMN2 dorsal SMN	0.203
Salience	DMN2 anterior DMN	0.184
DMN4 dorsal posterior precuneus	SMN2 dorsal SMN	0.122
DMN1 medial temporal	SMN2 dorsal SMN	0.121
CEN2 dorsal prefrontal	DMN3 precuneus/PCC	0.112
DMN4 dorsal posterior precuneus	SMN1 auditory SMN	−0.102
DMN2 anterior DMN	DMN3 precuneus/PCC	−0.105
CEN2 dorsal prefrontal	DMN2 anterior DMN	−0.133
DMN5 dorsal central precuneus	SMN1 auditory SMN	−0.143
Salience	DMN4 dorsal posterior precuneus	−0.151
DMN1 medial temporal	DMN2 anterior DMN	−0.151
DMN2 anterior DMN	DMN4 dorsal posterior precuneus	−0.165
SMN1 auditory SMN	CEN1 lateral frontoparietal	−0.171
CEN2 dorsal prefrontal	CEN3 subcortical	−0.208
CEN3 subcortical	CEN1 lateral frontoparietal	−0.221
Salience	CEN1 lateral frontoparietal	−0.265
DMN4 dorsal posterior precuneus	CEN3 subcortical	−0.356

Note: Only absolute weights >0.1 shown.
Abbreviations: CEN, central executive network; DMN, default mode network; PCC, posterior cingulate cortex; SMN, sensorimotor network; VIS, visual network.

TABLE 5 Sparse canonical correlation analysis for within-network resting-state functional connectivity: mode 1 and mode 3 weights for the behavioural variates

Measure	Weight mode 1	Weight mode 3
Social bias	0.881	
LOT pessimism	−0.472	−0.167
COS optimism		0.956
LOT optimism		0.242

Abbreviations: COS, Comparative Optimism Scale; LOT, Life Orientation Test-Revised.

Although mode 3 was also significant, its RR-score indicated that its reliability was less important (see Reliability section). Mode 3 optimism data weights were strongly driven by personal comparative optimism (weight = 0.96) and to a lesser degree by optimism as a trait (weight = 0.24; see Table 5). The RSFC variate was primarily driven by decreased connectivity within the CEN networks (CEN1: weight = −0.36; CEN2: weight = −0.26; CEN3: weight = −0.42) and within the SAL network (weight = −0.38) and increased WNFC within three DMN networks (DMN1: weight = 0.22; DMN4: weight = 0.20; DMN5: weight = 0.37) and the SMN (SMN2: weight = 0.40) and VIS (VIS1: weight = 0.25) (see Table 6).

4.1 | Reliability analyses

In order to ascertain that our results were not spurious and can likely be found in other studies, we performed several reliability analyses. First, using an alternative brain atlas (i.e., the CAREN atlas), we found that weights in all significant modes of all analyses correlated at $r > 0.95$ between the analyses (correlating weights for the CAREN atlas with those yielded in the primary analyses). Second, leave-one-out analyses indicated that the new recomputed variable weights correlated with the original weights (i.e., analyses with all the participants) at $r > 0.85$ for the all RSFC sCCA, $r > 0.84$ for the BNFC sCCA, and $r > 0.77$ for the WNFC sCCA. Third, bootstrapping and redrawing of the sample suggested that the overall sCCA correlation coefficients are stable at the size of the current sample (see Data S1 and Figure S1), particularly for the overall and the BNFC sCCAs. Lastly,

TABLE 6 Sparse canonical correlation analysis for within-network resting-state functional connectivity: mode 1 and mode 3 weights for the resting-state connectivity variates

Network	Weight Mode 1	Weight Mode 3
VIS2 medial occipital	0.214	−0.040
VIS1 lateral occipital	0.033	0.252
SMN1 auditory SMN	−0.081	0.110
CEN2 dorsal prefrontal	−0.149	−0.262
Salience	−0.162	−0.376
DMN4 dorsal posterior precuneus	−0.171	0.200
DMN3 precuneus/PCC	−0.196	0.070
CEN3 subcortical	−0.241	−0.422
CEN1 lateral frontoparietal	−0.291	−0.359
DMN5 dorsal central precuneus	−0.299	0.365
SMN2 dorsal SMN	−0.300	0.398
DMN1 medial temporal	−0.444	0.221
DMN2 anterior DMN	−0.557	−0.140

Abbreviations: CEN, central executive network; DMN, default mode network; PCC, posterior cingulate cortex; SMN, sensorimotor network; VIS, visual network.

mean RR-scores were as follows: all RSFC sCCA mode 1: mean RR = 0.65, BNFC sCCA mode 1: mean RR = 0.57, WNFC sCCA mode 1: mean RR = 0.76, analysis 2 mode 3: mean RR = 0.46.

5 | DISCUSSION

We investigated how social and personal optimism biases are related to RSFC across the brain. To do so, we performed three sCCAs. A simplified interpretation of the results of mode 1 can be seen in Figure 4. In a first analysis including all RSFC data, we found a significant and reliable mode that expressed the association of the optimism data with both BNFC and WNFC. Specifically, both personal and social optimism biases (the idea that good things are more likely to happen to oneself and others that one likes or identifies with) contributed positively to the mode's optimism variate, which in turn was associated with RSFC. At the same time, dispositional pessimism (the idea that things generally do not end well for oneself) contributed negatively. Because of the positive weights for different forms of optimism and negative weights for pessimism, this dimension could be called a generalised optimism dimension.

The first mode's RSFC variate was primarily driven by BNFC involving the CEN (commonly thought to be involved in tasks) and SAL (commonly thought to signify the importance and clarity of new information), as well as the DMN (commonly thought to reflect self-referential processing, being particularly active in the absence of active tasks). With one exception (BNFC between the lateral frontoparietal CEN network and the dorsal prefrontal CEN network), connectivity among the networks that belong to the CEN and SAL contributed negatively towards the generalised optimism dimension. Similarly, RSFC within and among networks of the DMN also contributed negatively. Together, these data suggest that reduced FC *within* networks involved in higher cognition (i.e., within the CEN/SAL networks and within the DMN) goes hand in hand with increased personal and social optimism. Decreased connectivity within networks is thought to reflect reduced functional specialisation (Ng, Lo, Lim, Chee, & Zhou, 2016). Correspondingly, reduced functional specialisation of each of these large-scale networks might be at the origin of people's enhanced positive outlook towards their own future and the futures of members that they associate with (i.e., well-liked groups). It may further be responsible for reducing personal pessimism.

Meanwhile, FC *between* the DMN subdivisions (task-negative), on the one hand, and the subdivisions of the CEN, SMN, and SAL networks (task-positive), on the other, mostly contributed positively. Increased connectivity between large-scale resting state networks may also be interpreted as reflecting reduced segregation, that is, reduced functional specialisation of the individual networks. In our study, such reduced segregation between these networks—although not uniformly—tended to associate with larger personal and social optimism biases and reduced personal pessimism. The subsequent findings of the sCCA focused solely on WNFC and the finding focused solely on BNFC are in line with this interpretation of all our RSFC data.
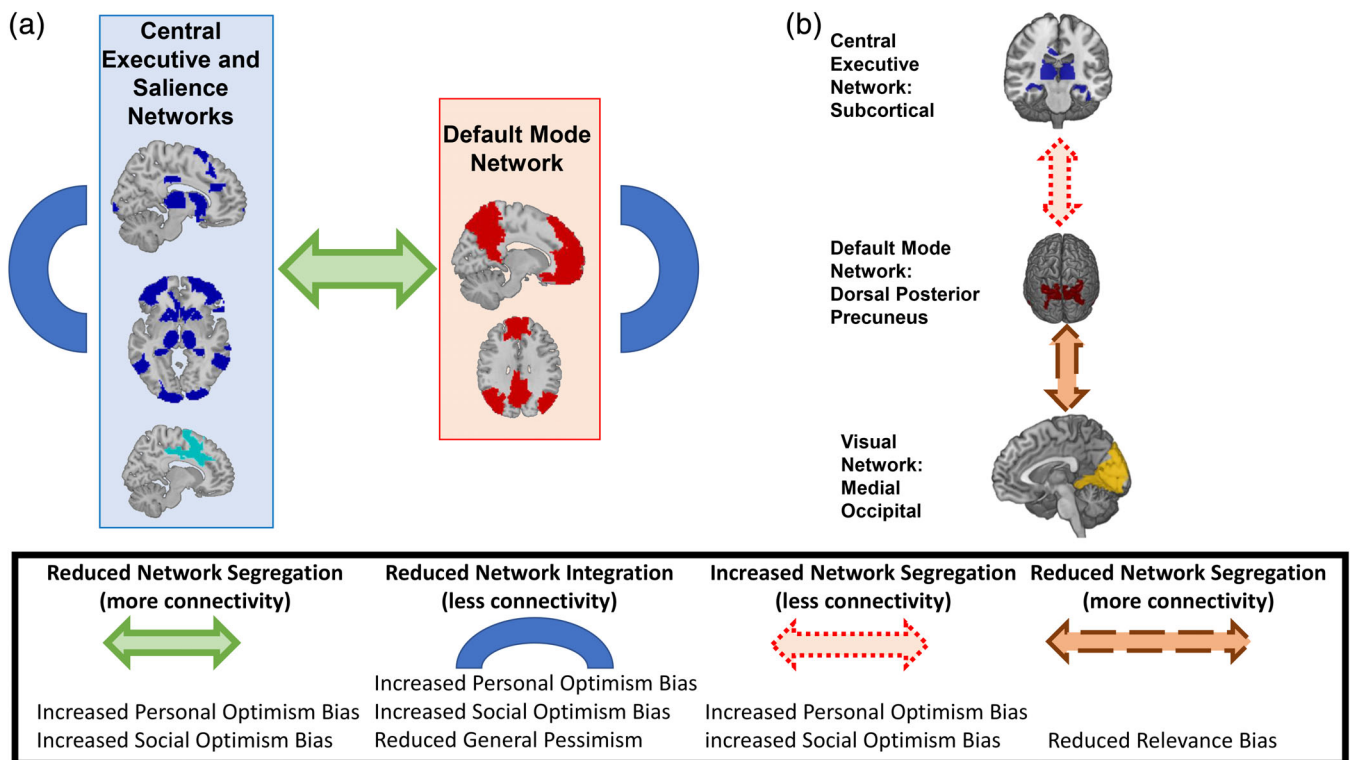

FIGURE 4 Cartoon of simplified interpretation of results connecting brain network connectivity to optimism and pessimism data. (a) Overall patterns of integration and segregation. (b) Specific connectivity pattern, including the dorsal posterior precuneus

The second sCCA, focusing on BNFC, largely replicated the findings described in Figure 4; that is, a general decreased segregation between and decreased integration within the CEN/SAL and the DMN was associated with increased optimism (both personal and social) and decreased pessimism. Concerning the sCCA using BNFC measures only, it is interesting to note that, although most of the strong indicators of network segregation in the present study were primarily situated in the SAL and in prefrontal regions, the strongest contribution was between the subcortical part of the CEN and the dorsal posterior precuneus subdivision of the DMN (see Figures 3 and 4b). Both of these networks are suggested to be earlier in the chain of stimulus processing than most other DMN and CEN networks (Kravitz, Saleem, Baker, & Mishkin, 2011; Saalmann & Kastner, 2011; Usrey & Alitto, 2015). Several regions of the subcortical CEN, for example, have an important role in the kind of emotion processing that could be conceptualised as precognitive (LeDoux, 2000) and involve spatial orientation and visual attention. Our finding is thus indicative of network segregation early in the processing stream. Such segregation may bias later higher cognition processing towards the creation of optimism biases by feeding forward information that involves a focus on specific predetermined aspects (i.e., information that one wants to be true) rather than on a more integrated overall perception. Correspondingly, we see the possibility that early selective attention sets the stage that allows for enhanced dwelling on desirable future outcomes. We recently demonstrated that, consistent with such an interpretation of our data, attention bias modification procedures can efficiently modify optimistic expectancies (Kress & Aue, 2019). Univariate correlations suggest that this particular early subcortical CEN-DMN connection revealed in our BNFC analysis is primarily associated with a valence bias (i.e., a general optimism bias that includes both social and personal optimism biases). This latter idea is supplemented by positive weights in the BNFC-focused sCCA for connectivity between the same parts of the DMN and the VIS and in the WNFC-focused sCCA in the VIS itself (see Figures 3 and 4b). Regions of the VIS are also likely to be early in the chain of processing, given their primary role in perception. Univariate analysis suggests that these findings are driven by a negative association of BNFC and relevance bias rather than by a valence bias. The combination of these results (as cartooned in Figure 4b) could be taken to mean that early sensory integration may be linked to a reduced focus on social versus individual relevance, which may be associated with early segregation of visual attention and spatial orientation, which in turn allows for generalisation of optimism biases from the individual to the group (i.e., a valence bias).

In the third sCCA focusing on WNFC, the first mode was driven by a strong social optimism bias, with dispositional personal pessimism contributing negatively. The RSFC variate, similar to the interpretation given in Figure 4, was driven by reduced connectivity within the DMN, SAL, and CEN. This latter finding may indicate that social (but not necessarily personal) optimism biases are associated with reduced cohesiveness in areas linked to higher cognition. This is further supported by post hoc univariate correlations, which were strongest negatively for the social bias and WNFC in three different DMN

subnetworks. On mode 3, in contrast, personal (but not social) optimism biases were significantly correlated with reduced cohesiveness in the CEN and SAL and increased cohesiveness of the DMN, SMN, and VIS. Mode 3 had lower reliability measures than did the other significant results, however, indicating that its interpretation needs to be taken with caution. Still, together, the two modes indicate that social optimism biases may be particularly divergent from personal optimism biases when it comes to WNFC. The fact that social optimism bias in WNFC (as revealed by mode 1) was solely paired with LOT pessimism (but no specific personal optimism measure) might indicate that the function of these social optimism biases may be particularly relevant to keep from becoming negative about one's own self (Aue et al., 2012).

Regarding the mechanisms underlying our findings as indicated in Figure 4a, we speculate that if a bias were to extend its influence on all cognitive processing modules, this would be easier to achieve if individual processing modules were not to function altogether independently from each other (i.e., if they are not overly segregated). Where processing is highly interdependent to start with, new biases affecting any network may propagate more easily across the entire higher order cognitive system.

Such an interpretation of our results would be in line with data on social stress, which has also been linked to reduced segregation between networks. A study revealed that following the stress of social exclusion, RSFC of the DMN with hubs of the SAL, in particular the anterior insula and the IFG, increased (Clemens et al., 2017). These findings are in accordance with the idea of stress being intimately linked with a stronger focus on short-term vigilance and habits over other forms of learning (Buckner, Dewall, Schmidt, & Maner, 2010; Wirz, Bogdanov, & Schwabe, 2018). Increased habitual thinking may be revealed in an increase in stereotypical thinking and thus be exemplified by increases in social (and personal) optimism biases.

Because of the associative nature of our study, inversed causality is an alternative interpretation: In order to propagate, biases may cause the reduction of modular brain network segregation. These alternatives are not necessarily mutually exclusive. If both directions of causality acted simultaneously, these two tendencies could reinforce each other; for example, stereotypical thinking of self and others could reduce modular processing independence, and reduced modular processing independence could render new biases more powerful, as all cognitive processes would be more likely to agree on their outcome.

A previous study found that WNFC in a pattern strongly overlapping with the SAL and posterior DMN (overlapping mostly DMN3 and some DMN1) was associated with higher reported emotional intelligence (Killgore et al., 2017). At the same time, BNFC between the SAL and both the anterior and posterior DMN was negatively correlated with reported emotional intelligence (Killgore et al., 2017). Together, the findings of this previous study point to emotional intelligence being linked to increased functional specificity in brain areas linked to higher cognition. Similarly, emotional intelligence has been linked to increased RSFC of a lateral parietal region within the DMN at large and decreased RSFC with the attention-related regions that

include parts of the VIS and SMN (Ling et al., 2019). The correspondence between these studies on reported emotional intelligence and the patterns found in the present study for optimism bias are noteworthy and point towards a common neural correlate, given the overlap between the two constructs (Bar-On, 2006).

Relatedly, several regions in the CEN and SAL and some in the DMN have been linked to empathy, as has the temporoparietal junction (Bzdok et al., 2012). Further, empathy has been related to RSFC patterns within parts of all three networks (SAL, DMN, and CEN) (Bilevicius, Kolesar, Smith, Trapnell, & Kornelsen, 2018). The strong overlap of our own results with the empathy network could arise because feeling with others (and taking their perspective) should reduce both overestimation of one's own prospects in comparison with others and negative stereotyping of members of disliked outgroups.

Lastly, it is noteworthy that personal and social optimism biases showed highly overlapping results in that they were situated at similar locations on the sCCA mode's variates in relation to the sCCAs for all RSFC and for BNFC. A previous study that used sCCA to investigate grey matter thickness also found a unified behavioural sCCA dimension that spanned both social and personal optimism (Moser et al., 2020). The present study therefore furthers the notion that the same biological underpinnings are shared between social and personal optimism biases. Hence, participants who have strong social optimism biases based on strong group identification may, at the same time, display a high degree of personal optimism bias and vice versa. Notably though, our WNFC analyses suggest that personal and social optimism biases are not necessarily identical in this regard.

Limitations: Participants' resting state scans were performed at variable intervals after they had performed the task (but always within 30 min). We therefore cannot exclude the possibility that the performance of the task had influenced their brain connectivity during the subsequent resting-state scan. Furthermore, despite the thorough reliability analyses undertaken in the present study, a higher number of participants would of course increase reliability. Although our additional analyses with a different atlas indicated that our results are reliable, we also note that there is spatial variability in atlases of the major resting-state networks that could lead to different interpretations (Doucet et al., 2019).

6 | CONCLUSIONS

When investigating associations between optimism and RSFC, we found that (a) reduced functional specificity among networks associated with higher cognition was associated with an optimism dimension of increased personal optimism and social optimism biases, but reduced personal pessimism. This was expressed as reduced segregation between and reduced cohesiveness/integration within the DMN and CEN/SAL networks. In addition, we found (b) a potential split in functional specificity in regions associated with perceptual and precognitive processing to be associated with the optimism dimension.

This was expressed as (a) connectivity of the dorsal precuneus with the subcortical CEN being associated primarily with a valence bias and (b) connectivity of the dorsal precuneus with the VIS being primarily associated with a relevance bias.

The present study's RSFC patterns—which indicate a link between optimism and reduced functional specificity—overlap with patterns observed in previous studies on emotional intelligence and empathy, where these concepts were broadly associated with increases in functional specificity. In this context, the reduced capacity to identify with members of disliked outgroups—both psychologically and biologically—may be related to a dampening of optimistic expectancies for these social targets, a hypothesis that remains to be tested in future studies.

An alternative interpretation is that increasing stereotypical thinking may be a mental shortcut to keep up personal optimism in the face of increased social stress that leads to habitual automatic thinking versus more complex deliberation. This preferential use of stereotypical thinking would then be represented in increased segregation of the DMN and CEN, especially during the early parts of processing. In this regard, one might also wonder whether individuals experiencing social stress on a regular basis may be more likely to display increased social optimism biases, a hypothesis that should also be examined in subsequent investigations.

Finally, our finding that optimism biases are linked to RSFC indicates that optimism biases are rooted in neurobiological processes that exist outside of concurrent tasks. This underlines the generalizability of the neural correlates of optimism biases and poses questions as to what the limits of the malleability of such biases may be.

DATA AVAILABILITY STATEMENT
The data that support the findings of this study are available as part of the supplemental data files or freely available online.

ORCID
Dominik Andreas Moser https://orcid.org/0000-0001-7119-1033
Mihai Dricu https://orcid.org/0000-0001-6155-2261
Raviteja Kotikalapudi https://orcid.org/0000-0003-4604-3367
Gaelle Eve Doucet https://orcid.org/0000-0003-4120-0474
Tatjana Aue https://orcid.org/0000-0001-9480-1711

REFERENCES

Andrews-Hanna, J. R. (2012). The brain's default network and its adaptive role in internal mentation. *The Neuroscientist*, *18*(3), 251–270. https://doi.org/10.1177/1073858411403316

Aue, T., Nusbaum, H. C., & Cacioppo, J. T. (2012). Neural correlates of wishful thinking. *Social Cognitive and Affective Neuroscience*, *7*(8), 991–1000. https://doi.org/10.1093/scan/nsr081

Bar-On, R. (2006). The Bar-On model of emotional-social intelligence (ESI). *Psicothema*, *18*(Suppl), 13–25.

Behzadi, Y., Restom, K., Liau, J., & Liu, T. T. (2007). A component based noise correction method (CompCor) for BOLD and perfusion based fMRI. *NeuroImage*, *37*(1), 90–101. https://doi.org/10.1016/j.neuroimage.2007.04.042

Bilevicius, E., Kolesar, T. A., Smith, S. D., Trapnell, P. D., & Kornelsen, J. (2018). Trait emotional empathy and resting state functional connectivity in default mode, salience, and central executive networks. *Brain Sciences*, *8*(7), 128. https://doi.org/10.3390/brainsci8070128

Bolton, T. A. W., Wotruba, D., Buechler, R., Theodoridou, A., Michels, L., Kollias, S., … Van De Ville, D. (2020). Triple network model dynamically revisited: Lower salience network state switching in pre-psychosis. *Frontiers in Physiology*, *11*, 66. https://doi.org/10.3389/fphys.2020.00066

Buckner, J. D., Dewall, C. N., Schmidt, N. B., & Maner, J. K. (2010). A tale of two threats: Social anxiety and attention to social threat as a function of social exclusion and non-exclusion threats. *Cognitive Therapy and Research*, *34*(5), 449–455. https://doi.org/10.1007/s10608-009-9254-x

Bzdok, D., Schilbach, L., Vogeley, K., Schneider, K., Laird, A. R., Langner, R., & Eickhoff, S. B. (2012). Parsing the neural correlates of moral cognition: ALE meta-analysis on morality, theory of mind, and empathy. *Brain Structure & Function*, *217*(4), 783–796. https://doi.org/10.1007/s00429-012-0380-y

Chowdhury, R., Sharot, T., Wolfe, T., Düzel, E., & Dolan, R. J. (2014). Optimistic update bias increases in older age. *Psychological Medicine*, *44*(9), 2003–2012.

Clemens, B., Wagels, L., Bauchmuller, M., Bergs, R., Habel, U., & Kohn, N. (2017). Alerted default mode: Functional connectivity changes in the aftermath of social stress. *Scientific Reports*, *7*, 40180. https://doi.org/10.1038/srep40180

Cordes, D., Haughton, V. M., Arfanakis, K., Carew, J. D., Turski, P. A., Moritz, C. H., … Meyerand, M. E. (2001). Frequencies contributing to functional connectivity in the cerebral cortex in "resting-state" data. *AJNR. American Journal of Neuroradiology*, *22*(7), 1326–1333.

Dolcos, S., Hu, Y., Iordan, A. D., Moore, M., & Dolcos, F. (2016). Optimism and the brain: Trait optimism mediates the protective role of the orbitofrontal cortex gray matter volume against anxiety. *Social Cognitive and Affective Neuroscience*, *11*(2), 263–271. https://doi.org/10.1093/scan/nsv106

Doucet, G. E., Lee, W. H., & Frangou, S. (2019). Evaluation of the spatial variability in the major resting-state networks across human brain functional atlases. *Human Brain Mapping*, *40*(15), 4577–4587. https://doi.org/10.1002/hbm.24722

Doucet, G. E., Rasgon, N., McEwen, B. S., Micali, N., & Frangou, S. (2018). Elevated body mass index is associated with increased integration and reduced cohesion of sensory-driven and internally guided resting-state functional brain networks. *Cerebral Cortex*, *28*(3), 988–997. https://doi.org/10.1093/cercor/bhx008

Dricu, M., Bührer, S., Hesse, F., Eder, C., Posada, A., & Aue, T. (2018). Warmth and competence predict overoptimistic beliefs for out-group but not in-group members. *PLoS One*, *13*(11), e0207670.

Dricu, M., Kress, L., & Aue, T. (2020). The neurophysiological basis of optimism bias. In T. O.-S. Aue Hadas (Ed.), *Cognitive biases in health and psychiatric disorders* (Vol. 1, pp. 41–70). Cambridge, MA: Academic Press.

Dricu, M., Schupbach, L., Bristle, M., Wiest, R., Moser, D. A., & Aue, T. (2020). Group membership dictates the neural correlates of social optimism biases. *Scientific Reports*, *10*(1), 1139. https://doi.org/10.1038/s41598-020-58121-4

Fox, M. D., Snyder, A. Z., Vincent, J. L., Corbetta, M., Van Essen, D. C., & Raichle, M. E. (2005). The human brain is intrinsically organized into dynamic, anticorrelated functional networks. *Proceedings of the National Academy of Sciences of the United States of America*, *102*(27), 9673–9678. https://doi.org/10.1073/pnas.0504136102

Friston, K. J., Williams, S., Howard, R., Frackowiak, R. S., & Turner, R. (1996). Movement-related effects in fMRI time-series. *Magnetic Resonance in Medicine*, *35*(3), 346–355. https://doi.org/10.1002/mrm.1910350312

Glaesmer, H., Hoyer, J., Klotsche, J., & Herzberg, P. Y. (2008). Die deutsche Version des Life-Orientation-Test (LOT-R) zum dispositionellen Optimismus und Pessimismus. *Zeitschrift für Gesundheitspsychologie*, *16*, 26–31.

Ing, A., Samann, P. G., Chu, C., Tay, N., Biondo, F., Robert, G., … Consortium, I. (2019). Identification of neurobehavioural symptom groups based on shared brain mechanisms. *Nature Human Behaviour*, *3*(12), 1306–1318. https://doi.org/10.1038/s41562-019-0738-8

Killgore, W. D. S., Smith, R., Olson, E. A., Weber, M., Rauch, S. L., & Nickerson, L. D. (2017). Emotional intelligence is associated with connectivity within and between resting state networks. *Social Cognitive and Affective Neuroscience*, *12*(10), 1624–1636. https://doi.org/10.1093/scan/nsx088

Kravitz, D. J., Saleem, K. S., Baker, C. I., & Mishkin, M. (2011). A new neural framework for visuospatial processing. *Nature Reviews. Neuroscience*, *12*(4), 217–230. https://doi.org/10.1038/nrn3008

Kress, L., & Aue, T. (2019). Learning to look at the bright side of life: Attention bias modification training enhances optimism bias. *Frontiers in Human Neuroscience*, *13*, 222. https://doi.org/10.3389/fnhum.2019.00222

LeDoux, J. E. (2000). Emotion circuits in the brain. *Annual Review of Neuroscience*, *23*, 155–184. https://doi.org/10.1146/annurev.neuro.23.1.155

Ling, G., Lee, I., Guimond, S., Lutz, O., Tandon, N., Nawaz, U., … Brady, R., Jr. (2019). Individual variation in brain network topology is linked to emotional intelligence. *NeuroImage*, *189*, 214–223. https://doi.org/10.1016/j.neuroimage.2019.01.013

Menon, V., & Uddin, L. Q. (2010). Saliency, switching, attention and control: A network model of insula function. *Brain Structure & Function*, *214*(5–6), 655–667. https://doi.org/10.1007/s00429-010-0262-0

Moser, D. A. (2018). Matlab code and example to calculate RR-score as related to Moser et al 2018 (Publication no. https://doi.org/10.13140/RG.2.2.33544.26883).

Moser, D. A., Doucet, G. E., Ing, A., Dima, D., Schumann, G., Bilder, R. M., & Frangou, S. (2017). An integrated brain-behavior model for working memory. *Molecular Psychiatry*, *23*, 1974–1980. https://doi.org/10.1038/mp.2017.247

Moser, D. A., Doucet, G. E., Lee, W. H., Rasgon, A., Krinsky, H., Leibu, E., … Frangou, S. (2018). Multivariate associations among behavioral, clinical, and multimodal imaging phenotypes in patients with psychosis. *JAMA Psychiatry*, *75*(4), 386–395. https://doi.org/10.1001/jamapsychiatry.2017.4741

Moser, D. A., Dricu, M., Wiest, R., Schupbach, L., & Aue, T. (2020). Social optimism biases are associated with cortical thickness. *Social Cognitive and Affective Neuroscience*, *15*, 745–754. https://doi.org/10.1093/scan/nsaa095

Moutsiana, C., Charpentier, C. J., Garrett, N., Cohen, M. X., & Sharot, T. (2015). Human frontal–subcortical circuit and asymmetric belief updating. *Journal of Neuroscience*, *35*(42), 14077–14085.

Ng, K. K., Lo, J. C., Lim, J. K. W., Chee, M. W. L., & Zhou, J. (2016). Reduced functional segregation between the default mode network and the executive control network in healthy older adults: A longitudinal study.

NeuroImage, *133*, 321–330. https://doi.org/10.1016/j.neuroimage.2016.03.029

Patel, A. X., Kundu, P., Rubinov, M., Jones, P. S., Vertes, P. E., Ersche, K. D., ... Bullmore, E. T. (2014). A wavelet method for modeling and despiking motion artifacts from resting-state fMRI time series. *NeuroImage*, *95*, 287–304. https://doi.org/10.1016/j.neuroimage.2014.03.012

Power, J. D., Barnes, K. A., Snyder, A. Z., Schlaggar, B. L., & Petersen, S. E. (2012). Spurious but systematic correlations in functional connectivity MRI networks arise from subject motion. *NeuroImage*, *59*(3), 2142–2154. https://doi.org/10.1016/j.neuroimage.2011.10.018

Raichle, M. E., MacLeod, A. M., Snyder, A. Z., Powers, W. J., Gusnard, D. A., & Shulman, G. L. (2001). A default mode of brain function. *Proceedings of the National Academy of Sciences of the United States of America*, *98*(2), 676–682. https://doi.org/10.1073/pnas.98.2.676

Ran, Q., Yang, J., Yang, W., Wei, D., Qiu, J., & Zhang, D. (2017). The association between resting functional connectivity and dispositional optimism. *PLoS One*, *12*(7), e0180334.

Saalmann, Y. B., & Kastner, S. (2011). Cognitive and perceptual functions of the visual thalamus. *Neuron*, *71*(2), 209–223. https://doi.org/10.1016/j.neuron.2011.06.027

Scheier, M. F., Carver, C. S., & Bridges, M. W. (1994). Distinguishing optimism from neuroticism (and trait anxiety, self-mastery, and self-esteem)—A reevaluation of the life orientation test. *Journal of Personality and Social Psychology*, *67*(6), 1063–1078. https://doi.org/10.1037/0022-3514.67.6.1063

Singh, L., Schupbach, L., Moser, D. A., Wiest, R., Hermans, E. J., & Aue, T. (2020). The effect of optimistic expectancies on attention bias: Neural and behavioral correlates. *Scientific Reports*, *10*(1), 6495. https://doi.org/10.1038/s41598-020-61440-1

Usrey, W. M., & Alitto, H. J. (2015). Visual functions of the thalamus. *Annual Review of Vision Science*, *1*, 351–371. https://doi.org/10.1146/annurev-vision-082114-035920

Wang, S., Zhao, Y., Cheng, B., Wang, X., Yang, X., Chen, T., ... Gong, Q. (2018). The optimistic brain: Trait optimism mediates the influence of resting-state brain activity and connectivity on anxiety in late adolescence. *Human Brain Mapping*, *39*(10), 3943–3955. https://doi.org/10.1002/hbm.24222

Weinstein, N. D. (1980). Unrealistic optimism about future life events. *Journal of Personality and Social Psychology*, *39*(806–820), 806–820. https://doi.org/10.1037/0022-3514.39.5.806

Wirz, L., Bogdanov, M., & Schwabe, L. (2018). Habits under stress: Mechanistic insights across different types of learning. *Current Opinion in Behavioral Sciences*, *20*, 9–16. https://doi.org/10.1016/j.cobeha.2017.08.009

Witten, D. M., Tibshirani, R., & Hastie, T. (2009). A penalized matrix decomposition, with applications to sparse principal components and canonical correlation analysis. *Biostatistics*, *10*(3), 515–534. https://doi.org/10.1093/biostatistics/kxp008

Wu, J., Dong, D., Jackson, T., Wang, Y., Huang, J., & Chen, H. (2015). The neural correlates of optimistic and depressive tendencies of self-evaluations and resting-state default mode network. *Frontiers in Human Neuroscience*, *9*, 618. https://doi.org/10.3389/fnhum.2015.00618

Yan, C. G., Wang, X. D., Zuo, X. N., & Zang, Y. F. (2016). DPABI: Data processing & analysis for (resting-state) brain imaging. *Neuroinformatics*, *14*(3), 339–351. https://doi.org/10.1007/s12021-016-9299-4

Yang, J., Wei, D., Wang, K., & Qiu, J. (2013). Gray matter correlates of dispositional optimism: A voxel-based morphometry study. *Neuroscience Letters*, *553*, 201–205. https://doi.org/10.1016/j.neulet.2013.08.032

Zhuang, X., Yang, Z., & Cordes, D. (2020). A technical review of canonical correlation analysis for neuroscience applications. *Human Brain Mapping*, *41*(13), 3807–3833. https://doi.org/10.1002/hbm.25090

SUPPORTING INFORMATION

Additional supporting information may be found online in the Supporting Information section at the end of this article.